Theoretical Studies on Hydration of Pyrrole, Imidazole, and Protonated Imidazole in the Gas Phase and Aqueous Solution

Peter I. Nagy,*,†,‡ Graham J. Durant,†,# and Douglas A. Smith*,§,†

Contribution from the Center for Drug Design and Development. Department of Medicinal and Biological Chemistry and Department of Chemistry, The University of Toledo, Toledo, Ohio 43606-3390

Received August 17, 1992

Abstract: Ab initio calculations using HF/6-31G* and MP2/6-31G* total geometry optimization were carried out in the gas phase for water, pyrrole, imidazole, and protonated imidazole monomers and various monohydrates of each organic. Optimized geometries for the ring systems are in good agreement with the experimental structures; normal frequencies are systematically overestimated. Using MP2/6-311++G** single point calculations, the gas-phase protonation free energy of imidazole was within 2.3 kcal/mol of the experimental value. Free energy calculations for the water–ring system complexes allowed us to estimate the relative populations of the monohydrates with different geometries. The in-plane hydration of pyrrole is preferred by 1.8 kcal/mol over the out-of-plane hydrated form. Imidazole is preferentially hydrated by 1.7 kcal/mol at N1 rather than at N3. The statistical perturbation method was used in Monte Carlo simulations to predict relative solvation energy terms. The relative solvation free energy of imidazole referred to pyrrole is –4.1 kcal/mol, and the relative solvation enthalpy is –10 to –12 kcal/mol. The hydrogen bond geometric parameters in solution are reasonably different from those in gas-phase monohydrates optimized using the OPLS interaction potential. The geometric parameters and relative energies for the monohydrates are closer to values obtained in the MP2 rather than HF ab initio calculations. The only remarkable difference between OPLS and MP2 results were found for the imidazole hydration at its N3 site. In dilute aqueous solution the pyrrole molecule forms a hydrogen bond of N–H···Ow type in the molecular plane. The neutral imidazole forms one in-plane N1-H···Ow hydrogen bond and one less localized hydrogen bond at the N3 site. There are also some water molecules located in the π-region which form weaker bonds to the solute. The protonated imidazole forms two strong in-plane hydrogen bonds of N-H···Ow type in aqueous solution with several water molecules in the π-region.

Introduction

Pyrrole and imidazole are simple representatives of heteroaromatics with basic nitrogen and/or acidic NH groups. They are building blocks of several biologically important organic molecules such as amino acids (tryptophan, histidine), nucleotide bases, indole alkaloids,[1] and histamine.[2] Owing to their importance, both molecules have been the subject of several investigations. Infrared and Raman spectra of pyrrole[3] and infrared spectra of imidazole[4] were determined in the gas phase and neat liquid. Molecular geometries were determined by microwave spectroscopy.[5,6] Ab initio calculations were carried out to obtain the normal frequencies for pyrrole[7] and for the gas-phase protonation energy of imidazole.[8]

Since these molecules exert their biologic effects in aqueous solution, studies of their hydration are of paramount importance. It is most surprising that there have been only a few theoretical investigations on the hydration of these five-membered rings. Monohydrates were investigated by ab initio calculations using the STO-3G basis set[9] and MINI-1 and 4-31G basis sets.[10,11] To our knowledge, however, no calculation simulating the dilute aqueous solutions of these solutes has been reported. Molecular dynamics simulations for aqueous solutions of proteins[12] having tryptophan or histamine residues or a recent simulation of tryptophan itself in water[13] concentrated mainly on conformational aspects. Crystal structure data for macromolecules with strongly bound water molecules[14] give the "frozen" position of the water oxygens, and their locations are strongly influenced by the chemical environment. The knowledge of the hydration pattern around the neutral and protonated imidazole would help to explain, for example, the role of the water binding to the Asp···His···Ser catalytic triad of serine proteases.[15]

Recently, one of us has reported Monte Carlo structure simulations for aqueous solutions of solutes containing the OH,

* To whom correspondence should be addressed.

† Center for Drug Design and Development and Department of Medicinal and Biological Chemistry.

‡ On leave from Chemical Works of Gedeon Richter Ltd., Budapest. Hungary.

Current address: Cambridge Neuroscience, One Kendall Square, Building 700, Cambridge, MA 02139.

§ Department of Chemistry.

(1) *The Chemistry of Heterocycles Compounds*; Weissberger, A., Taylor, E. C., Eds.; *John Wiley*: New York, 1983; Part IV, Vol. 25.

(2) Cooper, D. G.; Young, R. C.; Durant, G. J.; Ganellin, C. R. In *Comprehensive Medicinal Chemistry*; Pergamon Press: 1990; Vol. 3, pp 323–421.

(3) Navarro, R.; Orza, J. M. *An. Quim., Ser. A* **1983**, *79*, 557, 571; **1984**, *80*, 59; **1985**, *81*, 5.

(4) (a) Bellocq, A. M.; Perchard, C.; Novak, A.; Josien, M. L. *J. Chim. Phys. Phys.-Chim. Biol.* **1965**, *62*, 1334. (b) Perchard, C.; Bellocq, A. M.; Novak, A. *J. Chim. Phys. Phys.-Chim. Biol.* **1965**, *62*, 1344.

(5) Nygaard, L.; Nielsen, J. T.; Kirchheiner, J.; Maltesen, G.; Rastrup-Andersen, J.; Soerensen, G. O. *J. Mol. Struct.* **1969**, *3*, 491.

(6) Christen, D.; Griffiths, J. H.; Sheridan, J. *Z. Naturforsch., Teil A* **1981**, *36*, 1378.

(7) (a) Simandiras, E. D.; Handy, N. C.; Amos, R. D. *J. Phys. Chem.* **1988**, *92*, 1739. (b) Kofranek, M.; Kovar, T.; Karpfen, A.; Lischka, H. *J. Chem. Phys.* **1992**, *96*, 4464.

(8) (a) Mo, O.; de Paz, J. L. G.; Yanez, M. *J. Phys. Chem.* **1986**, *90*, 5597. (b) Lim, C.; Bashford, D.; Karplus M. *J. Phys. Chem.* **1991**, *95*, 5610.

(9) Del Bene, J. E.; Cohen, I. *J. Am. Chem. Soc.* **1978**, *100*, 5285.

(10) Alagona, G.; Ghio, C.; Nagy, P. *J. Mol. Struct.* (THEOCHEM) **1989**, *187*, 219.

(11) Alagona, G.; Ghio, C.; Nagy, P.; Simon, K.; Naray-Szabo, G. *J. Comput. Chem.* **1990**, *11*, 1038.

(12) (a) Van Gunsteren, W. F., Weiner, P. K., Eds. *Computer Simulations of Biomolecular Systems*; Escom: Leiden, 1989. (b) McCammon, J. A.; Harvey, S. C. *Dynamics of Proteins and Nucleic Acids*; Cambridge University Press: Cambridge, 1987.

(13) Gordon, H. L.; Jarrell, H. C.; Szabo, A. G.; Willis, K. J.; Somorjai, R. L. *J. Phys. Chem.* **1992**, *96*, 1915.

(14) Bernstein, F. C.; Koetzle, T. F.; Williams, G. T. B.; Mayer, E. F., Jr.; Brice, M. D.; Rogers, J. R.; Kennard, O. Shimanouchi, T.; Tasumi, M. *J. Mol. Biol.* **1977**, *112*, 535.

(15) Weiner, S. J.; Seibel, G. L.; Kollman, P. A. *Proc. Natl. Acad. Sci. U.S.A.* **1986**, *83*, 649.

0002-7863/93/1515-2912$04.00/0

Scheme I

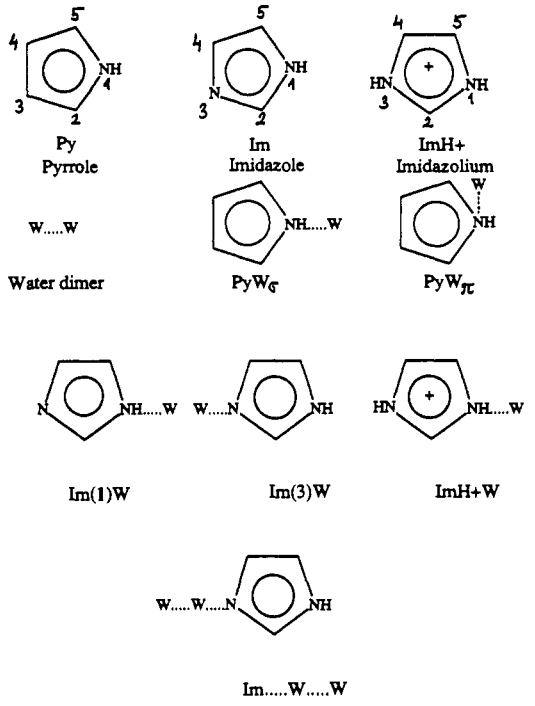

OCH_3, NH_2, $NHCH_3$, and CN functional groups.[16] Ab initio quantum chemical calculations and statistical perturbation theory[17,18] were applied to estimate the conformational equilibria for 1,2-ethanediol[19] and 2-hydroxybenzoic acid[20] in aqueous solution. To facilitate our ongoing study for the equilibrium of the histamine tautomers and conformers in aqueous solution,[21] we have first investigated the hydration of the heterocyclics themselves. Identification of the hydration pattern at the aromatic basic nitrogen and the aromatic NH group will be of use in the analysis of structures having other polar sites as well.

Published theoretical and experimental results for the hydrations of these aromatics are limited. Imidazole is an amphoteric molecule in aqueous solution with a pK_a of 6.7, while pyrrole is acidic with $pK_a = 0.3$.[22] The estimated free energy of hydration is about −4 kcal/mol for the neutral imidazole and about −60 kcal/mol for the protonated form.[23] No such data could be found for pyrrole.

The relatively small amount of information on the hydration thermodynamics and the solution structure of these molecules further justify our interest in this field. Ab initio geometry optimization and normal frequency analyses have been carried out for the monomers (water, pyrrole, neutral and protonated imidazole) and for the organic monohydrates. Estimates of the protonation energy of the imidazole and the free energies of formations for the monohydrates in the gas phase were obtained. Monte Carlo studies provided the relative hydration free energy of pyrrole referred to imidazole. Finally we analyzed the hydrogen bond structure and the average solvent arrangement around pyrrole, imidazole, and imidazolium cation in aqueous solution.

Table I. Optimized Geometries for Pyrrole and for Neutral and Protonated Imidazole[a]

	pyrrole			imidazole			imidazoleH$^+$	
	HF	MP2	exp[b]	HF	MP2	exp[c]	HF	MP2
				R/Å				
N1C2	1.363	1.372	1.370	1.349	1.365	1.364	1.313	1.338
C2X3[d]	1.358	1.381	1.382	1.289	1.324	1.314	1.313	1.338
X3C4[d]	1.427	1.417	1.417	1.372	1.375	1.382	1.381	1.375
C4C5	1.358	1.381	1.382	1.350	1.376	1.364	1.340	1.370
C5N1	1.363	1.372	1.370	1.372	1.374	1.377	1.381	1.375
N1H	0.992	1.011	0.996	0.993	1.012	0.998	1.000	1.018
C2H	1.070	1.081	1.076	1.071	1.082	1.079	1.069	1.080
X3H[d]	1.071	1.082	1.077				1.000	1.018
C4H	1.071	1.082	1.077	1.070	1.081	1.078	1.068	1.079
C5H	1.070	1.081	1.076	1.068	1.080	1.079	1.068	1.079
				Angles/deg				
512	109.5	110.1	109.8	106.8	107.6	106.9	109.5	110.4
123	108.2	107.4	107.7	112.2	111.6	112.0	108.0	106.5
234	107.1	107.5	107.4	105.3	104.9	104.9	109.5	110.4
345	107.1	107.5	107.4	110.5	111.0	110.7	106.5	106.4
451	108.2	107.4	107.7	105.2	104.9	105.5	106.5	106.4
H12	125.3	124.9		126.5	126.4		124.7	124.2
H23	130.8	131.4		125.6	125.9		126.0	126.8
H34	126.9	126.8					125.8	125.4
H45	126.0	125.6		128.1	127.8		131.3	131.0
H51	121.1	121.2		122.4	122.3		122.2	122.6

[a] HF and MP2 mean HF/6-31G* and MP2/6-31G* basis sets for the geometry optimization. [b] Reference 5. [c] Reference 6. [d] X3 is carbon for pyrrole and N for imidazole. For angles three-digit numbers refer to the heavy atoms of the ring. For numbering the aromatic rings, see Scheme I. For the angles, e.g., H12, the numbers 12 refer to the ring atoms 1 and 2.

Methods and Calculations

Ab initio quantum chemical calculations for the gas-phase monomers (water, pyrrole, neutral and protonated imidazole) and hydrates were carried out by utilizing Gaussian 90 package[24] running on a Stardent Titan 3040 computer at the University of Toledo and on a Cray Y-MP8 at the Ohio Supercomputer Center. We considered, as hydrates, the water dimer, two pyrrole···water dimers, two imidazole···water dimers, the imidazoleH$^+$···water dimer, and the imidazole···water···water trimer (Scheme I).

The monomer and dimer geometries were optimized both at HF and MP2 levels using the 6-31G* basis set.[25] Dimer geometries with rigid monomers were also optimized using the OPLS potential function.[26] The trimer was optimized only at HF level. Each HF/6-31G* optimization and, for the monomers, the MP2/6-31G* optimizations were followed by normal frequency analysis to make sure an energy minimum was obtained and for calculating free energies at 298 K and 1 atm. In the free energy calculations the thermal correction to the enthalpy, $H(T)$, and entropy, $S(T)$, were calculated in the rigid-rotor, harmonic oscillator approximation. Ideal gas behavior was accepted in the imidazole protonation reaction and for the formation of monohydrates. The thermal energy contributions were calculated using classical statistical thermodynamics functions.[27] The total entropy for PyWπ and Im(3)W without any molecular symmetry contain a term of RT ln 2 due to the entropy of mixing.

To estimate the basis set superposition error, BSSE, for the dimerization energies at MP2/6-31G*//MP2/6-31G* level, counterpoise calculations were carried out using the method of Boys and Bernardi.[28] Applying the definition equation of Sokalski et al.,[29] BSSE was obtained as the difference of the monomer energies calculated in the monomer and the dimer basis

(16) (a) Nagy, P. I.; Dunn, W. J., III; Nicholas, J. B. *J. Chem. Phys.* **1989**, *91*, 3707. (b) Dunn, W. J., III; Nagy, P. I. *J. Phys. Chem.* **1990**, *94*, 2099. (c) Dunn, W. J., III; Nagy, P. I. *J. Comput. Chem.* **1992**, *13*, 468.
(17) Zwanzig, R. W. *J. Chem. Phys.* **1954**, *22*, 1420.
(18) Jorgensen, W. L.; Ravimohan, C. *J. Chem. Phys.* **1985**, *83*, 3050.
(19) (a) Nagy, P. I.; Dunn, W. J., III; Alagona, G.; Ghio, C. *J. Am. Chem. Soc.* **1991**, *113*, 6719. (b) Nagy, P. I.; Dunn, W. J., III; Alagona, G.; Ghio, C. *J. Am. Chem. Soc.* **1992**, *114*, 4752.
(20) Nagy, P. I.; Dunn, W. J., III; Alagona, G.; Ghio, C. *J. Phys. Chem.* **1993**, in press.
(21) Nagy, P. I.; Durant, G. J.; Hoss, W.; Smith, D. A. To be published.
(22) (a) *Handbook of Chemistry and Physics*, 61st ed.; Weast, R. C., Ed.; CRC Press: Boca Raton, FL, 1980–81. (b) Perrin, D. D. *Dissociation Constant of Organic Bases in Aqueous Solution*, Suppl. 1; Butterworths, London, 1972.
(23) Pearson, R. G. *J. Am. Chem. Soc.* **1986**, *108*, 6109.
(24) Gaussian 90, Revision J: Frisch, M. J.; Head-Gordon, M.; Trucks, G. W.; Foresman, J. B.; Schlegel, H. B.; Raghavachari, K.; Robb, M.; Binkley, J. S.; Gonzalez, C.; Defrees, D. J.; Fox, D. J.; Whiteside, R. A.; Seeger, R.; Melius, C. F.; Baker, J.; Martin, R. L.; Kahn, L. R.; Stewart, J. J. P.; Topiol, S.; Pople, J. A. Gaussian, Inc.: Pittsburgh, PA, 1990.
(25) (a) Hariharan, P. C.; Pople, J. A. *Theor. Chim. Acta* **1973**, *28*, 213. (b) Hehre, W. J.; Radom, L.; Schleyer, P. v. R.; Pople, J. A. *Ab Initio Molecular Orbital Theory*; John Wiley: New York, 1986.
(26) Jorgensen, W. L., Tirado-Rives, J. *J. Am. Chem. Soc.* **1988**, *110*, 1657.
(27) McQuerrie, D. *Statistical Mechanics*; Harper and Row: New York, 1976.
(28) Boys, S. F.; Bernardi, F. *Mol. Phys.* **1970**, *19*, 553.
(29) Sokalski, W. A.; Roszak, S.; Hariharan, P. C.; Kaufman, J. J. *Int. J. Quantum Chem.* **1983**, *23*, 847.

Table II. Optimized Geometric Parameters Calculated Using the 6-31G* Basis Set for Hydrates

	PyWσ			Im(1)W			ImH⁺ W		
	HF	MP2	OPLS	HF	MP2	OPLS	HF	MP2	OPLS
				R/Å					
N1–H	0.998	1.019	1.011	0.999	1.021	1.012	1.015	1.043	1.018
O–H	0.948	0.969	0.957	0.948	0.970	0.957	0.950	0.971	0.957
(N1)H···O	2.066	1.952	1.792	2.030	1.922	1.774	1.806	1.705	1.684
N1···O	3.064	2.971	2.803	3.029	2.943	2.786	2.821	2.747	2.702
				Bond Angles/deg					
C2NC5	109.2	109.7	110.1	106.6	107.1	107.6	109.2	109.8	110.4
HOH	106.3	104.9	104.5	106.3	105.0	104.5	106.3	105.6	104.5
N1–H···O	178.9	179.1	179.6	179.9	179.9	178.4	178.0	176.4	179.5
				Torsion Angles/deg					
ON1C2C5	179.5	179.8	180.0	179.9	179.7	180.0	178.9	179.8	180.0
HwON1C5	85.4	65.7	85.3	92.3	67.3	89.9	85.7	82.3	90.8
	−85.8	−65.8	−85.3	−92.1	−67.1	−89.9	−86.8	−82.7	−90.8
	PyWπ			Im(3)W			ImWW		
	HF	MP2	OPLS	HF	MP2	OPLS	HF	MP2	OPLS
				R/Å					
N1–H	0.993	1.011							
O–H	0.949	0.972		0.954	0.979	0.957	0.960		
	0.949	0.968		0.947	0.969	0.957	0.947		
N···O[a]	3.571	3.274		2.974	2.881	2.880	2.930		
N··Hw[a]	3.021	2.701		2.102	1.995	1.923	2.002		
	3.444	3.298							
				Bond Angles/deg					
CNC[a]	109.6	110.2		105.7	105.5	104.9	105.8		
HOH	103.9	102.3		104.8	103.3	104.5	105.8		
H–N1···O	106.5	103.1							
N3···H–O				151.2	149.6	176.7	161.8		
				Torsion Angles/deg					
ONC2C5	75.6	76.3							
HwONH	−127.2	−137.9							
	107.2	107.8							
ON3C2N1				178.8	178.1	140.7	178.3		
HwN3C2N1				175.5	175.0	139.4	−179.5		
				−165.9	−165.5	155.3	162.5		

[a] N is N1 for pyrrole and N3 for imidazole.

sets. Since the monohydrate geometries are fully optimized in our calculations, the question arose whether to use the optimized monomer geometries or the monomer geometries optimized in the dimer. In the former case the relative location of the real and ghost orbitals is not unambiguous. Thus we chose the second way. Though the sum of the energies of monomers (with geometry obtained in the dimer) were higher by about 0.1 kcal/mol than the minimal energies, the small geometry changes were thought to result in a negligible effect on BSSE calculated as a difference of molecular energies in two bases with the same geometry. For the ImH⁺W system, where the largest increase in the energy was found due to changes in the geometries, calculations with both sets of monomer geometries were carried out. In defining the location of the ghost orbitals with optimized monomers geometries, the H atom, H-N1 bond direction, and the HN1C5 plane were superimposed for ImH⁺, the O atom, the HOH bisector, and the molecular plane for water. The calculated change in BSSE was 0.02 kcal/mol.

Single point calculations were carried out at MP2/6-31G*//HF/6-31G* and MP2/6-311++G**//MP2/6-31G* levels. Calculated optimized geometries for pyrrole (Py), imidazole (Im), and protonated imidazole (ImH^+) are compared with experimental values in Table I. Optimized geometric parameters for the Py···W, Im···W, Im···W···W, and ImH^+···W hydrates are given in Tables II and some structures are shown in Figure 1. Calculated normal frequencies are given in Table III. Energy results are summarized in Tables IV and V.

The structures of the dilute aqueous solutions of pyrrole, imidazole, and protonated imidazole were studied by Monte Carlo simulations using the BOSS 3.1 program of Jorgensen.[30] The program was adapted here to run on the Stardent Titan 3040 computer. The details of calculations for N, P, T ensembles have been described by Jorgensen et al.[31]

In the present simulations the OPLS potential function was used utilizing the parameterization of Jorgensen and Tirado-Rives for the peptide side chains.[26] There are united CH atom parameters for the rings in His and Trp, and the same charges are given for the ring N and attached H atoms in both residues. (It is remarkable that the ring parameters were fitted in a series where pyridine and pyrrole represented the rings with aromatic N and NH atoms, respectively. Thus the imidazole parameters come from values fitted for aromatics with a *single* nitrogen in the ring system.) Our calculated N as well as H Mulliken charges in pyrrole and imidazole are similar taking either the HF or MP2 optimized structures: e.g., q(N) values are −0.701 and −0.711 in pyrrole and imidazole, respectively, at the MP2 level. The corresponding q(H) values, 0.393 and 0.403, indicate a slightly more polar N–H bond in imidazole but the same overall charge for the NH group. Also the C(2)H group in pyrrole and the corresponding C(5)H group in imidazole bear (summed) charges of 0.222 and 0.200, respectively. Thus using the same charges for the N, H, and C(2)H atoms in pyrrole and for the corresponding atoms in imidazole seems reasonable. Maintaining the C_{2v} symmetry for pyrrole results in charges of −0.055 for C(3)H and C(4)H atoms, in agreement with the value of Jorgensen and Tirado-Rives.[26] Their parameters for the neutral and protonated imidazoles were accepted without further consideration. Molecular geometries were obtained from optimizations at the MP2/6-31G* level, and are in good agreement with the experimental geometric parameters for the neutral species (Table I): therefore, the ImH^+ structure was considered also reliable.

Thus six- and seven-point models were used for the neutral and ionic solutes in the Monte Carlo simulations. The TIP4P model was applied for the water:[32] 262 water molecules were considered in a box with a single solute in the center at $T = 298$ K and $P = 1$ atm. Periodic boundary conditions and preferential sampling,[33] proportional to $1/(R^2 + c)$, were applied where R is the distance of the solvent molecule from the center of the N–N axes of the solutes (N–C3 for pyrrole) and c is a constant

(30) Jorgensen, W. L. *User's* Manual for the BOSS Program Version 3.1.
(31) (a) Jorgensen W. L.; Madura, J. D. *J. Am. Chem. Soc.* **1983**, *105*, 1407. (b) Jorgensen W. L.; Swenson, C. *J. Am. Chem. Soc.* **1985**, *107*, 1489. (c) Jorgensen W. L.; Gao, J. *J. Phys. Chem.* **1986**, *90*, 2174.
(32) (a) Jorgensen W. L.; Chandrasekhar, J.; Madura, J. D.; Impey, R. W.; Klein, M. L. *J. Chem. Phys.* **1983**, *79*, 926. (b) Jorgensen, W. L.; Madura, J. D. *Mol. Phys.* **1985**, *56*, 1381.
(33) (a) Owicki, J. C.; Scheraga, H. A. *Chem. Phys. Lett.* **1977**, *47*, 600. (b) Jorgensen W. L. *J. Phys. Chem.* **1983**, *87*, 5304.

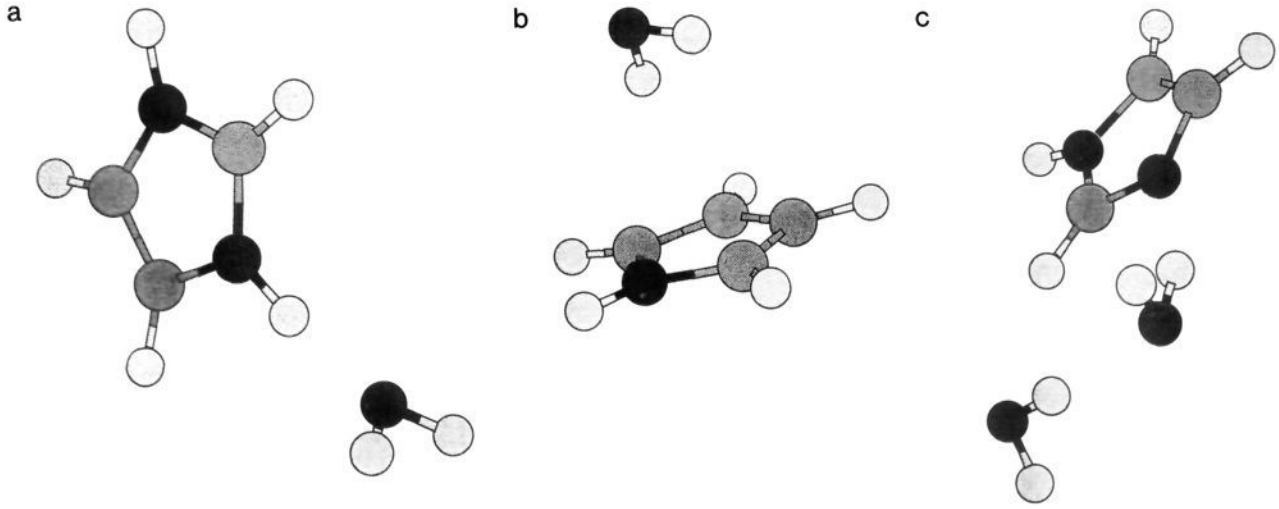

Figure 1. (a) Optimized structure of the imidazolium cation···water complex (ImH^+W). (b) Optimized structure of the pyrrole···water complex with out-of-plane hydration ($PyW\pi$). (c) Optimized structure of the imidazole···water···water trimer (ImWW).

Table III. Calculated Normal Frequencies for the Heterocycles Using the 6-31G* Basis Set

	pyrrole			imidazoleH^+			imidazole		
	HF	MP2	exp[a]	HF	MP2		HF	MP2	exp[b]
a_1	968	904	880	1010	946	a″	536	527	517
	1110	1071	1018	1174	1135		693	641	612–626
	1161	1136	1074	1226	1178		734	686	660–667
	1264	1196	1148	1329	1233		839	693	723
	1548	1473	1391	1632	1491		965	772	809
	1641	1542	1470	1795	1639		999	819	930–965
	3430	3304	3125	3488	3350				
	3455	3324	3148	3508	3361				
	3926	3686	3527	3856	3620	a′	985	906	855–870
							1022	946	890–905
b_2	946	881	863	991	923		1158	1107	1055
	1166	1097	1049	1042	1100		1192	1130	1065–1083
	1253	1201	1134	1294	1227		1235	1180	1120–1135
	1437	1339	1287	1450	1370		1258	1202	1260
	1595	1522	1424	1596	1509		1411	1302	1320–1340
	1744	1601	1521	1716	1607		1505	1402	1390–1415
	3417	3293	3116	3489	3345		1588	1496	1465–1495
	3449	3318	3140	3848	3613		1666	1538	1530
							1745	1570	1590–1630
a_2[c]	679	592	618	674	619		3445	3308	3140
	806	639	712	749	712		3447	3313	3140
	1000	796	868	1017	835		3475	3336	3160
							3921	3674	3518
b_1	484	470	474	671	640				
	684	641	626	799	740				
	830	712	720	863	765				
	966	778	826	1139	830				

[a] Reference 3. [b] Reference 4. [c] Experimental a_2 frequencies for pyrrole are from Raman spectroscopy for the liquid.

Table IV. Dimer Interaction Energies Calculated at Different Theoretical Levels[a]

	HF/ 6-31G*	MP2/ 6-31G*	MP2/ 6-311++G**	MP2/ 6-31G* BSSE	OPLS
$PyW\sigma$	−5.36	−7.56	−6.78	−5.78	−7.18
$PyW\pi$	−3.72	−6.03	−5.63	−3.08	
Im(1)W	−6.36	−8.56	−7.56	−6.78	−8.27
Im(3)W	−7.06	−9.68	−7.43	−5.94	−5.55
ImH^+W	−16.94	−20.27	−18.14	−18.33	−16.74

[a] Geometries are optimized at HF/6-31G* level in the HF calculations and at MP2/6-31G* level in all MP2 calculations. OPLS interaction energies were obtained by optimization with rigid TIP4P water and aromatic rings fixed at the MP2 optimized geometries (cf. Table I).

set equal to 120. Solute–solvent and solvent–solvent cutoff radii were taken as 9.75 Å and 8.50 Å, respectively. New configurations due to random translation and rotation of the solute were tried in every 50th step. Volume changes were attempted in every 1000th step. Statistical averages were taken over separate runs of 100K configurations; 4500K configurations were considered in the equilibration phases and 4500–6000K configurations in the averaging phases producing distribution functions used in solution structure analyses.

Table V. Calculated Free Energy Changes for Gas-Phase Protonation and Hydration[a]

$B + H^+ = BH^+$

B	ΔE	0.9*ΔZPE	ΔH(T)	$T\Delta S$(T)	ΔG	ΔG(exp)[b]
imidazole	−231.62	8.41	−1.48	−8.12	−216.57	−214.3

$B + H_2O = B{\cdot}H_2O$

$B{\cdot}H_2O$	ΔE	0.9*ΔZPE	ΔH(T)	$T\Delta S$(T)	ΔG
$PyW\sigma$	−6.78	1.02	0.38	−4.87	−0.51
$PyW\pi$	−5.63	1.14	0.20	−5.60	1.31
Im(1)W	−7.56	1.13	0.29	−5.91	−0.22
Im(3)W	−7.43	1.86	−0.25	−7.33	1.52
ImH^+W	−18.14	1.57	−0.16	−7.20	−9.52

[a] Energy changes in kcal/mol. ΔE values from MP2/6-311++G**//MP2/6-31G* calculations. ZPE, H(T), and S(T) values were calculated using HF/6-31G*//HF/6-31G* frequencies. [b] The more recent value of ΔH = −222.1 kcal/mol from ref 38a was taken. Then in calculating ΔG(exp), the procedure in refs 38b and 8b was followed: $\Delta G = \Delta H + TS_{prot}$, where the value of 7.8 kcal/mol[39] was taken for TS_{prot}. Comments in ref 38a indicate that the error in the proton affinity, and thus in ΔG, is estimated to be ±1–2 kcal/mol.

Relative thermodynamic data were obtained by using the statistical perturbation method.[17,18] Using a linear coupling (λ) for the geometric and OPLS parameters, pyrrole (λ = 0) was transformed through nonphysical intermediate states to imidazole (λ = 1). Forward and backward simulations were carried out considering intermediate states with λ = 0.25, 0.50, 0.75, and 0.875. In these calculations 3000K and 4500K configurations were considered in the equilibration and averaging phases, respectively (Table VI).

In interpreting the simulation results for solution structures snapshots (Figure 2 and 7), energy pair distributions functions (Figure 3) and radial distribution functions (Figures 4–6) were applied.[16,19] Statistical averaging of the solvent positions with reference to the solute[19a] was used for the imidazole solute; 4000 snapshots of the solution structure from 6000K configurations were analyzed. The average positions of the water oxygen and hydrogen atoms were located meeting any distance requirements Ow···N <3.5 Å, Ow···C <4.5 Å, Hw···N <2.5 Å. Calculated coordination numbers, numbers of hydrogen bonds, and average solute–solvent intermolcular geometric parameters are given in Tables VII–IX.

Results and Discussion

Geometries. Optimized geometries for the aromatic rings in the gas phase are shown in Table I. All molecules were assumed planar, with imposed C_{2v} symmetry on pyrrole and protonated imidazole. Calculated bond lengths are considerably different

Table VI. Relative Free Energy, Enthalpy, and Entropy of Imidazole to Pyrrole in Aqueous Solution

λ_i	λ_j	$\Delta G_{i\to j}$	$\Delta H_{i\to j}$	$T\Delta S_{i\to j}$	$\Delta G_{j\to i}$	$\Delta H_{j\to i}$	$T\Delta S_{j\to i}$
0.000	0.250	−0.47(0.03)	−0.40(0.37)	0.07(0.36)	0.55(0.04)	1.98(0.54)	1.44(0.53)
0.250	0.500	−0.78(0.05)	−2.35(0.64)	−1.57(0.63)	0.68(0.06)	2.64(0.64)	1.96(0.64)
0.500	0.750	−1.04(0.07)	−5.51(0.99)	−4.47(0.96)	1.04(0.09)	4.89(0.94)	3.85(0.94)
0.750	0.875	−0.75(0.04)	−2.37(0.48)	−1.61(0.31)	0.85(0.03)	0.80(0.33)	−0.05(0.32)
0.875	1.000	−0.98(0.03)	−0.99(0.34)	−0.01(0.33)	1.02(0.03)	0.29(0.30)	−0.73(0.30)
total changes		−4.02(0.10)	−11.61(1.37)	−7.59(1.29)	4.14(0.12)	10.60(1.34)	6.46(1.33)

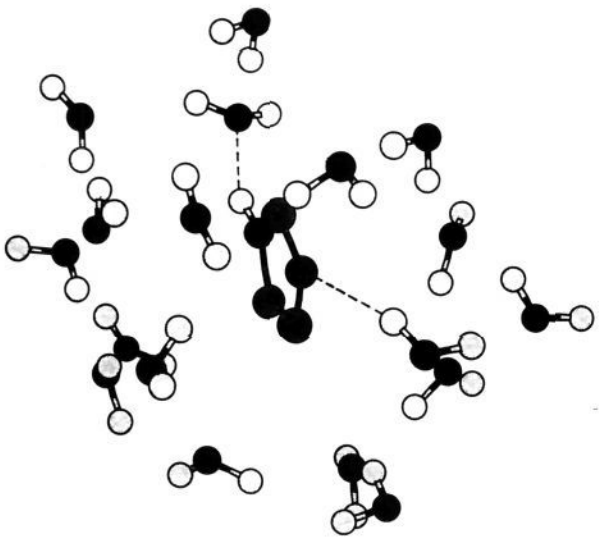

Figure 2. Snapshot for the closest environment of the imidazole solute in dilute aqueous solution. Hydrogen bonds are indicated by dashed lines.

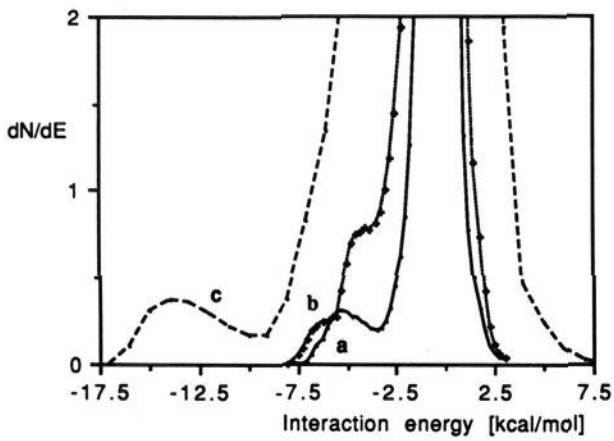

Figure 3. Energy pair distribution functions of the solute–solvent interaction in aqueous solution: (a) pyrrole (solid line), (b) imidazole (marked dotted line), (c) imidazolium cation (dashed line.)

when using the HF versus MP2 methods, and the signs of the differences do not show a general tendency. In contrast to the bond lengths, the bond angles are close to each other calculated at the two levels.

MP2 calculated geometric parameters are closer to the experimental values than the HF ones. The agreement is very good for the pyrrole ring geometry, and the only considerable difference between the MP2 calculations and experiment is that the N–H bond length is overestimated by about 0.02 Å. The experimental C–H bond lengths are inbetween the two theoretically predicted sets. Though the agreement with the experimental values is not as good for imidazole as for pyrrole, MP2 corrected much of the deficiencies of HF in this case also. At the MP2 level the seriously underestimated HF C2N3 distance is corrected even though the bond length is somewhat longer now than the experimental value. In general, the MP2 predicted ring geometry is close to the experimental, since the bond angles are also in good

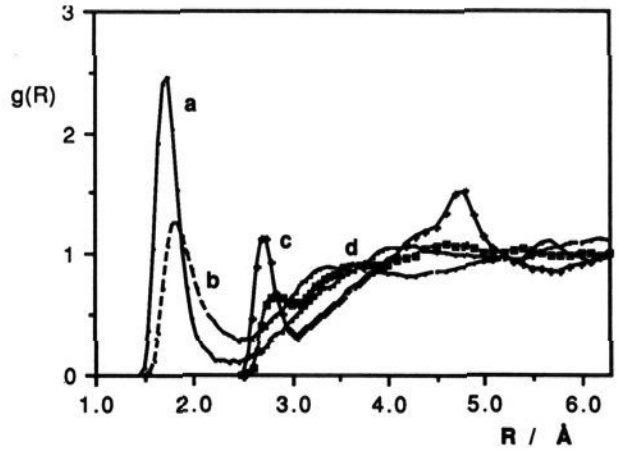

Figure 4. Radial distribution functions for pyrrole and the imidazolium cation in aqueous solution H···Ow: (a) imidazolium (solid line), (b) pyrrole (dashed line); N···Ow: (c) imidazolium (marked solid line), (d) pyrrole (squared line).

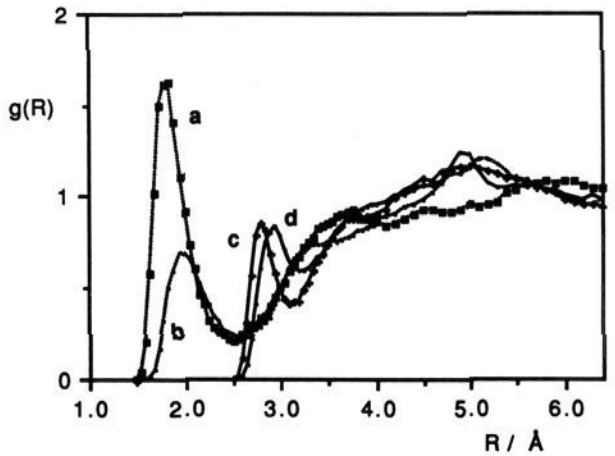

Figure 5. Radial distribution functions for imidazole in aqueous solution: (a) (N1)H···Ow (marked dotted line), (b) N3···Hw (dotted line), (c) N1···Ow (marked solid line), (d) N3···Ow (solid line).

Table VII. Number of Hydrogen Bonds and Solute–Solvent Interaction Energies[a]

	conf number	H-bond no. (E_{ul})	E_{SX}
pyrrole	4500K	0.8 (−3.50)	−17.0(±0.2)
imidazole	4500K	1.8 (−3.50)	−26.8(±0.3)
	6000K	1.9 (−3.50)	−26.3(±0.3)
ImH^+	4500K	2.0 (−9.00)	−118.6(±0.7)
			−135.4(±0.7)[b]

[a] (E_{ul}) indicates the upper limit of integration in the energy pair distribution function. [b] Value obtained using Born correction.

agreement. The N–H length is overestimated similarly to the case of the other aromatics, but it is properly predicted both at the HF and MP2 levels that this distance is longer in imidazole than in pyrrole.

There is no experimental geometry for the protonated imidazole. The calculated MP2 values do not indicate dramatic changes in comparison to the neutral form. The bond lengths in the ring

Table VIII. Characteristic Points of the Radial Distribution Functions and Coordination Numbers in Aqueous Solution

	N1···Ow	N1···Hw	H1···Ow	N3···Hw	N3···Ow	C2···Ow	C4···Ow
			Pyrrole				
R_{start}	2.55	1.90	1.55			2.90	2.95
R_{max}	2.85	3.60	1.85			3.75	3.90
R_{min}	3.10	4.10	2.50			5.00	4.65
coord no.	1.0	11–12	1.0			14	11
			Imidazole				
R_{start}	2.55	2.05	1.50	1.65	2.60	2.90	2.95
R_{max}	2.80	3.15	1.85	1.95	2.95	3.75	3.70
R_{min}	3.10	3.45	2.50	2.60	3.25	4.55	4.30
coord no.	1.0	4.0	1.1	1.4	1.4	10	7
			ImidazoleH$^+$ [a]				
R_{start}	2.50	2.55	1.45			2.90	2.85
R_{max}	2.70		1.75			3.60	3.70
R_{min}	3.05		2.40			4.60	4.50
coord no.	1.1		1.0			10	9

[a] Average N1···Ow and H1···Ow values from the two equivalent sets of radial distribution functions.

Table IX. Average Geometric Parameters of the Hydrogen Bonds to Imidazole in Aqueous

	distances						
	H···Ow	N···Hw	N···Ow	N···H···O	tors angle NCNO	pop. Ow, %	pop. Hw, %
N3C2N1H···Ow	1.81		2.82	172	−174	64	
N1C2N3···HwOw		2.03	2.98	171	142	31	20
N3C2N1H···Ow	3.33		3.58	96	130	25	
	3.11		3.45	101	−114	26	
				N···OwHw	C2N1OwHw		
C2N1H···OwHw		3.16		106	160	64	26

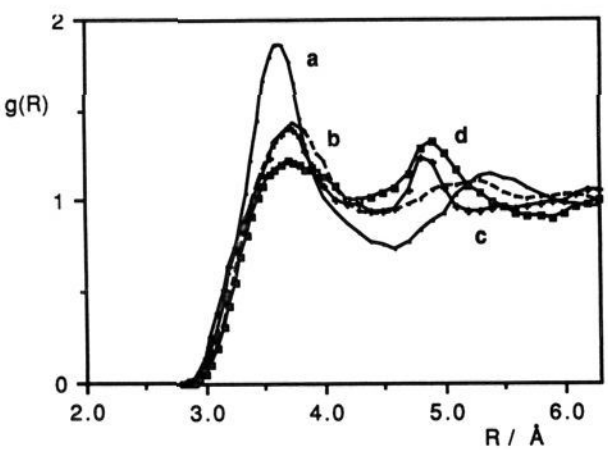

Figure 6. Radial distribution functions in the nonpolar regions of the neutral and protonated imidazole: (a) imidazolium C2···Ow (solid line), (b) imidazole C2···Ow (dashed line), (c) imidazolium C4···Ow (marked solid line), (d) imidazole C4···Ow (squared solid line).

Figure 7. Snapshot for the closest environment of the protonated imidazole solute in dilute aqueous solution. Hydrogen bonds are indicated by dashed lines.

become more uniform with small corresponding changes in the bond angles. The N–H and C–H bond lengths increase and decrease, respectively, by some thousanths of an angstrom when compared to neutral form. There are negligible changes for the HXC (X = N, C) bond angles.

Some of the geometric parameters of the hydrated species are given in Table II. No experimental values have been reported for these structures. The rings have changes of 0.001–0.003 Å in the bond lengths and of no more than 0.6° in the bond angles as compared to the nonhydrated structures.

For complexes with a N–H···Ow hydrogen bond, the N–C bond lengths are consistently shorter and the CNC angles are larger than those in the free bases at both the HF and MP2 levels. The N–H bond lengths undergo the largest increase by about 0.006 and 0.009 Å for the neutral molecules and 0.015 Å and 0.025 Å for the protonated species at the two levels. The O–H bond lengths and HOH angles show only a small variation in these complexes, and the values are close to those in the free water (O–H = 0.947 and 0.969 Å, HOH = 105.5 and 104.0° at HF and MP2 levels, respectively).

Considering the intermolecular geometric parameters, the H···Ow distance decreases for the PyWσ, Im(1)W, and ImH+W series as 2.066, 2.030, 1.806 Å (HF) and 1.952, 1.922, 1.705 (MP2). The N–H···Ow angles show only little changes at the two levels. Thus taking the electron correlation into account, the bond lengths are much more affected than bond angles, a result similar to that found for the free bases.

The H(N) and Ow atoms lie in the ring planes and the water hydrogens are symmetrically above and below the planes. The N···O vector and the HOH bisector make an angle of 174°–177° at the HF level and 144°–170° at the MP2 level. The complexes have C_s symmetry within the precision of symmetry unconstrained calculations. (An HF calculation for PyWσ with constrained C_{2v} symmetry resulted in a transition structure with one negative frequency.) Considering electron correlation, the HOH plane in the Im(1)W complex is declined toward C5 rather than C2 atom, contrary to the HF results. Though there may not be a simple explanation, it seems likely that the large positive charges on the C2-H2 atoms make proximity to this side of the ring unfavorable

for the water hydrogens. The importance of the electrostatic effect is clear in the case of the imidazolium cation. The water hydrogens point away from C2 neighboring the other N–H group. Instead, the Hw atoms point toward the less positive region around C5, as the value of the HONC5 torsion angle <90° indicates.

π-Hydration of pyrrole with the entire water molecule on the same side of the ring plane leaves the N–C and N–H bond lengths almost unaltered at both levels. While the CNC angle remains almost unchanged, the H(N) atom moves out of the plane toward the water. The water oxygen is nearly in the vertical symmetry plane of the pyrrole with an H–N···Ow angle of 103°–106°. The locations of the hydrogens are, however, asymmetric (see HwO···NH torsion angles) with increased bond lengths compared to the unbound water. The HOH angles decreased by 1.6°–1.7°. This is contrary to the σ-hydrogen bonded cases where the HOH angles for the acceptor water molecules have increased. The N···O distance for the π-complex is considerably decreased from its HF value of 3.57 Å to 3.27 Å at the MP2 level. Correspondingly, the shorter N···Hw hydrogen bond distance for the π-complex is also reduced from 3.02 Å to 2.70 Å, giving an even more asymmetric optimized structure at the MP2 level. Thus calculations for the π-hydration of pyrrole predict a bifurcated structure with two nonequivalent water hydrogens.

Attempts to find monohydrates with π-complexation failed for imidazole and the imidazolium cation. Total geometry optimization starting from structures found as minima in partial geometry optimizations for imidazole–water complexes[10,11] led to arrangements with water oxygen in the ring plane. Thus we considered a dihydrated imidazole where the first water was placed in the ring plane hydrating the N3 site. The second water molecule with a bifurcating orientation in the π-region moved to the ring plane, hydrogen bonding to the first water molecule upon full optimization. Normal frequency analysis proved that this structure is a local energy minimum. Lowrey and Williams[34] found in hydration calculations for methylamine that the third water molecule does not hydrate the third, unsolvated polar site of methylamine. Instead, it is bridging two water molecules hydrogen bonded to them. In the case of imidazole hydration it is energetically preferred to form a strong water–water hydrogen bond instead of a presumably less stable π-complex to the aromatic ring. Also, no stable π-complex was found for the cation. Starting from different arrangements in the π-region, the water moved either to the stable in-plane position or gave a transition-state structure with a nearly C_{2v} symmetry.

In imidazole hydrates with donor water, the bond lengths change by no more than 0.003 Å in the ring system for Im(3)W. The increase in the C2N3C4 angle is a few tenths of degree. An increase of 0.006 Å for the N3–C2 bond length in ImWW indicates, however, a considerable solvent effect. This effect becomes even more evident when considering the changes in the water geometry and differences for the intermolecular geometric parameters.

The water O–H in hydrogen bond to N3 in Im(3)W is considerably stretched as compared to the other, "free" O–H bond that remains the same as in a separate water molecule. An increase of the bond length in the proton donor molecule is general as was found for $(H_2O)_2$,[35a] HOH···NH_3[35b] or for hydrogen halide complexes.[35c] A further stretching was calculated for ImWW at HF level (0.960 Å versus 0.954 Å) when a second water also takes part in the hydration. The H–O–H angle decreases for the monohydrate, but the value for the dihydrate, 105.4°, is close to that in the isolated water molecule (105.5°).

The N3···Hw distance decreases as much as 0.1 Å at the HF level when the second water molecule is considered. The N3···H–O angle increases by 10° to 162° leaving the hydrogen bond still bent. Even though the MP2 optimization for the monohydrate, Im(3)W, resulted in a decrease of about 0.11 Å for the N3···Hw distance in comparison with the HF value (a decrease similar to that found for the H···O for PyWσ and Im(1)W), the MP2 optimized angle for the hydrogen bond remained close to the HF value. This result suggests that the bent N3···H–O bond for the monohydrate, calculated at the HF level, is not due to the lack of considering the electron correlation. The change in the bond angle when considering a second water molecule is due to other reasons.

The N3···H(Ow) bond in the monohydrate is longer than the (N1)H···Ow bonds (Table II), but becomes shorter for the dihydrate. The decrease is due to the arrangement of the second water molecule in the C2 region. Since there is a large positive atomic charge on C2, a single water molecule has an optimal orientation when the O atom is moved toward this region. As a consequence, the N3···Hw distance in Im(3)W increases and the N3···H–O angle declines from linearity by 30°. When there is a second water (ImWW), it can locate at the C2 site allowing the first water molecule to form a stronger (shorter and more linear) hydrogen bond to N3.

Torsion angles, close to 180°, show that the O–H bond directed to imidazole is only slightly out of the plane of the ring, in contrast to the nonhydrogen bonded water hydrogen. The different signs for the torsion angles for the water hydrogens indicate a bifurcated arrangement. Torsion angles change little in the dihydrate. The HwN3C2N1 angle almost reaches 180° in this system, indicating that the in-plane hydration is favored over the slightly bifurcated arrangement in the monohydrate. Nonetheless, the above findings suggest that the N3 region is not superior to its neighbors to strongly locate a single water molecule in the ring plane with a nearly linear hydrogen bond. This is contrary to the N1–H region of imidazole or pyrrole.

OPLS optimizations with rigid monomer geometries (MP2 structures for the rings and TIP4P water) found energy minima for PyWσ, Im(1)W, Im(3)W, and ImH^+W. PyWπ is not a local energy minimum on the pyrrole–water potential surface using OPLS interaction potential function. Starting from several arrangements (close to or farther from the ab initio optimized structure), the dimer geometry moved to a PyWσ structure.

H···Ow and N1···Ow distances are shorter by 0.02–0.17 Å than the MP2 values for PyWσ, Im(1)W, and ImH^+W (Table II), but follow the tendency found in the ab initio calculations. N1–H···Ow angles are close to 180°, the water oxygens are in the ring plane, and water hydrogens are symmetrical above and below the plane. The HOH bisector is almost coinciding with the N1–Ow vector for the three dimers.

Much larger differences from the ab initio results were found for Im(3)W. Though the N3···Hw distance is consistently smaller than the MP2 value by 0.07 Å, the N3···H–O bond is close to linear resulting in an N3···Ow distance equal to the MP2 value. More serious is that the O atom is out of the ring plane by as much as 40°. Thus the OPLS potential favors the largely out-of-plane hydration over the in-plane one, in contrast to the ab initio results. It should be noted here, however, that the potential surface is very soft for the Ow···N3C2N1 torsion using the OPLS function. The interaction energy with an in-plane water, that is, when Ow···N3C2N1 is equal to 180°, is less negative only by 0.05 kcal/mol than the minimal energy value. If the Ow···N3C2N1 torsion angle is equal to 90°, the energy increases by 1.7 kcal. These energy values predict that the imidazole ring can by hydrated at the N3 site in aqueous solution with a wide range of the Ow···N3C2N1 torsion angle.

Vibrational Frequencies. While there are two recent frequency calculations for the pyrrole, we have not found high-level ab initio frequency results for imidazole. Simandiras et al.[7a] using double-ζ MP2 calculations found frequencies close to the present ones. The average overestimation of their calculated frequencies referred to the experiment is 3.8% compared with the present value of 3.9% (Table III). Very close agreement to the experimental values

(34) Lowrey, A. H.; Williams, R. W. *J. Mol. Struct. (THEOCHEM)* **1992**, *253*, 35.

(35) (a) Frisch, M. J.; Pople, J. A.; Del Bene, J. E. *J. Phys. Chem.* **1985**, *89*, 3664. (b) Del Bene, J. E. *J. Comput. Chem.* **1989**, *10*, 603. (c) Hannachi, Y.; Silvi, B. *J. Mol. Struct.* (THEOCHEM) **1989**, *200*, 483.

was obtained by Kofranek et al.[7b] using a basis set of double-ζ quality and applying scaled force constants.[36] Since in the present calculations the main aim is to find a consistent scaling factor to be used for correcting the zero-point vibration energy, it is not of primary interest if our calculated values are overestimated. The HF frequencies are overestimated for the pyrrole by 10.8%, and the HF/MP2 overestimation ratio is 1.067. HF and MP2 calculations for imidazole overestimate the frequencies on average by 9.6% and 2.2%, respectively. The HF/MP2 overestimation ratio is 1.072 for the neutral imidazole and 1.068 for its protonated form. Thus the frequencies consistently decrease when going from HF to MP2 calculations. Since only HF values were calculated for the hydrates, an average scaling factor of 0.9 based on the above results was accepted for those complexes. This value is also acceptable for scaling the water frequencies where the overestimation is 12.0%.

While the overestimation of the frequencies at HF level could be checked for the isolated molecules, there are no experimental data for the vibrational frequencies of the hydrates. The calculated N–H and O–H stretching frequencies for bonds involved in hydrogen bonds in the hydrates show an expected red shift of about 80 cm^{-1} for the neutral and 280 cm^{-1} for the ionic species from their values in the free molecules. It is hard to estimate, however, how correct the low frequencies describing the intermolecular vibrations are. The frequencies of the intermolecular vibrations are generally less than 400 cm^{-1} for these systems calculated at HF/6-31G* level. To check the effect of the basis set, frequencies for the water dimer were calculated here to compare the 6-31G* results with those obtained with larger basis sets.[35a,37] Both the HF and MP2 results are in fair agreement with their counterparts. Since the largest contribution to the vibrational enthalpy and entropy comes from the low-energy modes that are considerably excited at 298 K, their precise calculation is important if free energies of dimerization are to be estimated. This raises the question whether to apply a general scaling factor to frequencies when calculating the thermal corrections. Free energy calculations for the 1,2-ethanediol showed[19] that, despite some frequencies calculated as less than 400 cm^{-1} for all conformers, the relative enthalpies and entropies differed by 0.02 kcal/mol using scaled or nonscaled frequencies. Following this, no scaling was applied in calculating the thermal corrections, but a scaling factor of 0.9 was used to calculate the zero-point energy correction. Because of the remaining uncertainties, however, we are interested in the present paper rather in relative than absolute values when comparing free energies of hydrates with different geometric arrangements (PyWσ versus PyWπ, Im(1)W versus Im(3)W).

Gas-Phase Energetics. Energy results are summarized in Tables IV–V. MP2/6-31G*//HF/6-31G* calculations for the hydration and protonation reactions (not indicated in the tables) give a roughly constant 0.3–0.6 kcal/mol increase in the energy changes, ΔE, as compared to the corresponding MP2/6-31G*//MP2/6-31G* values. This suggests that the $\Delta\Delta E$ values, the relative energy changes for the hydration reactions in Table IV, are only moderately affected whether the geometry optimization was taken at the HF or MP2 level. The change of 0.26 kcal/mol for the protonation energy is negligible relative to the MP2/6-31G*//MP2/6-31G* value of −234.20 kcal/mol.

The effect of the basis set on ΔE is more important. The calculated gas-phase protonation free energy of imidazole (Table V), using our highest level, MP2/6-311++G**//MP2/6-31G* estimation for ΔE at 0 K, is −216.6 kcal/mol. To our knowledge this is the best theoretical estimate of this value, which is known to be −214.3 kcal/mol based on experiment[38] (see footnote in Table V.) Using the smaller basis but the same geometries, zero-point, and thermal energy corrections, the MP2/6-31G*//MP2/6-31G* calculated free energy of protonation is −219.2 kcal/mol.

The effect of the different basis sets and/or consideration of the electron correlation on the relative hydration energies can be assessed based on data in Table IV. The HF/6-31G*//HF/6-31G* values are less negative by 2.2–2.6 kcal/mol than the MP2/6-31G* values but show the same tendency for the neutral monohydrates. For the ionic species the decrease in the binding energy is 3.3 kcal/mol. Using the MP2/6-311++G** basis set, the dimerization energies become also less negative by 0.4-2.3 kcal/mol relative to the MP2/6-31G* values. Because of the different shift of the energies, however, the relative hydration energies are considerably different with the two basis set. The in-plane hydration of pyrrole, PyWσ, is favored over PyWπ by 1.5 and 1.2 kcal/mol by these basis sets. In contrast, while Im-(3)W is favored over Im(1)W by 1.1 kcal/mol using the MP2/6-31G* basis, Im(1)W is the more stable arrangement by 0.1 kcal when using the MP2/6-311++G** basis. These results suggest that energies obtained with the MP2/6-31G* basis set have not converged. The energy values may suffer a considerable basis set superposition error. Furthermore, the estimation of the relative binding energy for Im(3)W seems to be the question most dependent on the basis set used for the series under study here.

The BSSE corrected MP2/6-31G* energies for the different dimers are given in Table IV. For dimers with acceptor water, the BSSE values are consistently 1.8–2.0 kcal/mol. These values are very close to 1.9 kcal/mol found by Frisch et al.[40] for the water dimer. With donor water the BSSE is 3.0 kcal/mol for PyWπ and 3.7 kcal/mol for Im(3)W. The HF/6-31G* results in Table IV are close to the BSSE corrected MP2/6-31G* values with the exception of the dimerization energy for Im(3)W. Considering, however, the estimated BSSE of about 1 kcal/mol for the water dimer[40] at the HF/6-31G* level, the difference in the binding energies for both BSSE corrected sets should be increased. The MP2/6-311++G**//MP2/6-31G* single point binding energies are between the BSSE uncorrected and corrected MP2/6-31G* values. The counterpoise results are often considered as an approximate upper bound to the BSSE.[41] According to this, the MP2/6-311++G** binding energies are overestimated by 0.8–2.5 kcal/mol for the neutral species. The BSSE corrected limit of the dimerization energy, however, depends on the basis set used to determine the BSSE value. In their study Frisch et al.[40] pointed out that the calculated binding energy for the water dimer decreases by a further 0.7 kcal/mol when the basis set is much larger than the 6-31G* set and the correlation effect is considered at MP4 instead of MP2 level. Thus it is not surprising that our MP2/6-311++G** binding energy value for the ionic dimer is slightly less than the BSSE corrected MP2/6-31G* value.

Because of the remaining uncertainties indicated above, the usefulness of BSSE corrected values was contested.[40,42] Instead, using a satisfactorily large basis set, BSSE uncorrected binding energies lead to excellent agreement with the experimental dimerization enthalpy for water.[40] Difficulties in calculating correct free energies in the hydration reactions are manyfold. The 6-311++G** basis used in our single point calculations is not considered to have reached the satisfactorily extended level. The thermal corrections are of comparable magnitude as the quantum mechanically calculated energy changes. While the translational and rotational energy and entropy corrections are nearly constant for these dimerizations, the vibrational energy

(36) Pulay, P.; Fogarasi, G.; Pang, F.; Boggs, J. *J. Am. Chem. Soc.* **1979**, *101*, 2550.
(37) Dykstra, C. E. *J. Chem. Phys.* **1989**, *91*, 6472.
(38) (a) Meot-Ner, M.; Liebman, J. F.; Del Bene, J. E. *J. Org. Chem.* **1986**, 51, 1105. (b) Lias, S. G.; Liebman, J. F.; Levin, D. *J. Phys. Chem. Ref. Data* **1984**, *13*, 695.
(39) Stull, D. R.; Prophet, H. *JANAF Thermochem. Tables* **1971**, NSRDS-NBS-37.
(40) Frisch, M. J.; Del Bene, J. E.; Binkley, J. S.; Schaefer, H. F. III *J. Chem. Phys.* **1986**, *84*, 2279.
(41) (a) Newton, M. D.; Kestner, N. R. *Chem. Phys. Lett.* **1983**, *94*, 198. (b) Kestner, N. R.; Newton, M. D.; Mathers, T. L. *Int. J. Quantum Chem. Symp.* **1983**, *17*, 431.
(42) Schwenke, D. W.; Truhlar, D. G. *J. Chem. Phys.* **1985**, *82*, 2418.

and entropy corrections are 2–3 and 5–7 kcal/mol, respectively. Because the H and TS terms are of the opposite signs when calculating the free energy, the vibrational thermal corrections amount to −2.5 to −4.3 kcal/mol. These values are 30–60% of the ΔE values for the neutral species. (The overall positive thermal correction is mainly due the large translational entropy term.) The uncertainties due to estimating the vibrational frequencies in the harmonic approximation allow only a crude estimation of the free energy of dimerization at 298 K. Thus, the equilibrium concentrations of 57% and 43%, calculated for PyWσ and Im(1)W in the B + H_2O = B···H_2O reaction, respectively, must be taken with caution. It is more reliable to compare ΔG values referring to different geometric arrangements of the same chemical system. Thus, the in-plane hydration at the N–H site is dominant both for pyrrole and imidazole over the out-of plane and N3 site hydrations, respectively. No such a comparison is possible for hydration of the imidazolium cation. The large negative value, −9.52 kcal/mol, for the free energy of formation of the hydrate suggests, however, that the equilibrium is fully shifted toward the complex form. This is in accord with the expectation for ion hydration in the gas phase.

Qualitative results for the hydration of pyrrole provide support for our above conclusions. Molecular beam studies,[43] studies of the electronic excitation spectra[44] of indole and fluorescence spectra of 7-azaindole,[45] both of which have a condensed pyrrole ring, find possible in-plane hydration and hydration in the π-region. Tubergen and Levy[44] mention the in-plane complex as usually more abundant.

A close analogue to PyWπ is the benzene–water 1:1 complex studied recently by microwave spectroscopy and theoretical calculations.[46] Water was found above the benzene ring in the complex with both hydrogens pointing toward the π-cloud. The distance of the centers of masses for the monomers, R, was found 3.35 Å experimentally, and the C_2 axes of the water makes an angle of θ = 20 ± 15° with the C_6 axes of benzene. MP2/6-31G** calculations give values R = 3.20 Å and θ = 24°. Calculated dimerization energies are 4.21 kcal/mol without and 1.78 kcal/mol with BSSE correction. In our MP2/6-31G* optimized PyWπ structure R = 3.08 Å and θ = 36°. (θ was defined here as the angle between the water bisector and the normal vector of the ring plane.) From Table IV the BSSE uncorrected and corrected binding energies are 6.03 and 3.08 kcal/mol. Structural data comparing the benzene–water and the pyrrole–water π complexes indicate the effect of the ring heteroatom. Both dimers have a bifurcated water but with asymmetric hydrogens with pyrrole in contrast to benzene. The calculated R value is smaller for PyWπ, and the water is more declined from the normal vector of the ring plane. The binding energy is larger by 1.3–1.8 kcal than for the benzene complex.

The last system to be discussed is the dihydrated complex of imidazole. For this complex only MP2/6-31G*//HF/6-31G* energies were calculated. The energy change at 0 K for the Im + water = Im(3)W reaction is −9.32 kcal/mol, and the energy change for Im(3)W + water = ImWW reaction is −13.88 kcal/mol! The water dimerization energy at the same level is −7.14 kcal/mol; thus the binding of the second water molecule may not be considered as a simple formation of a water···water chain. Figure 1c shows that the second water is located close to the C2–H2 bond. H2···Ow and C2···Ow distances are 2.38 Å and 3.33 Å, respectively, considerably less than the corresponding sums of the van der Waals radii of 2.6 Å and 3.4 Å.[22a] The possibility for C–H···O hydrogen bonds in crystals was shown previously based on data basis search for imidazole containing compounds[11] and was recently investigated theoretically for methane–water complexes.[47] In the Im(3)W hydrate the Mulliken charges for the C2 and H2 atoms are 0.282 and 0.240, respectively. The corresponding charges in the dihydrate are 0.267 and 0.284. The considerable increase of the positive charge on the H2 atoms favors the formation of a weak hydrogen bond or at least an electrostatic stabilization with the second water molecule having a net charge of −0.015. Table II shows a decrease of the N3···Hw distance by 0.1 Å. This dramatic change makes this hydrogen bond stronger, also contributing to the large stabilization energy upon the binding of the second water molecule.

The interaction energies obtained by using OPLS potential are shown in Table IV. The relative dimerization energies for PyWσ and Im(1)W and the dimerization energy for ImH$^+$W were predicted close to the ab initio values. The relative stability of the Im(3)W dimer is underestimated as compared with the ab initio results. Indeed, the largest deviation from the ab initio geometries were found also for Im(3)W. The differences in the geometries and relative stabilities for Im(3)W seem to indicate some subtle effect in forming the N3···H–O hydrogen bond that was unable to be considered in the OPLS parameterization.

Solution Structure Simulations. When simulating the solution structures for pyrrole and imidazole, statistical perturbation calculations were carried out to estimate the relative solvation free energy, enthalpy, and entropy. Table VI shows the results for the forward and backward simulations. The average values for imidazole relative to pyrrole were ΔG = −4.08(±0.08), ΔH = −11.1(±1.0), $T\Delta S$ = −7.0(±0.9). The relative enthalpy of solvation calculated directly from the difference of the enthalpies of the solutions is −14.0(± 3.6) kcal/mol. This predicted range of ΔH and the one obtained in the perturbation calculations can be consistently satisfied by a relative solvation enthalpy range of −10.4 to −12.1 kcal/mol. The corresponding entropy changes are −6.3 to −8.0 kcal/mol.

Snapshots of the solution structures around the solutes are given in Figures 2 and 7 for the neutral and protonated imidazole. Though they show instantaneous arrangements in the solution, they are representative of many of the following findings.

Energy pair distribution functions for pyrrole and neutral imidazole are shown in Figure 3. There is a single maximum for pyrrole and there are two shoulders for imidazole. The range between −7.0 and −3.5 kcal/mol for the pyrrole–water interaction covers the ab initio values −6.8 and −5.6 kcal/mol, calculated for PyWσ and PyWπ, respectively, in the gas phase. The onset of the curve, that is, the most negative solute–solvent interaction energy found in the solution simulation, is at a slightly less negative value than the OPLS optimized interaction energy of the pyrrole–water dimer, −7.2 kcal/mol. The shoulder between −8.0 and −6.0 kcal/mol for imidazole fits nicely to the ab initio imidazole–water interaction energies of about −7.5 kcal/mol for the in-plane hydrations in gas phase. The OPLS calculated optimal Im(1)W interaction energy, −8.3 kcal/mol, explains the onset of the distribution function at about −8.0 kcal/mol. Also the shoulder between −5.0 and −3.5 kcal/mol is well explained by considering the OPLS optimized interaction energy of −5.5 kcal for Im(3)W.

Integrating the energy distribution function for pyrrole from −8.0 kcal/mol to its minimum at −3.5 kcal/mol gives 0.8, the number of water molecules in hydrogen bond the solute (Table VII). The same integration for imidazole up to the end of the second shoulder gives about 1.8 hydrogen bonds. The solute–solvent interaction energies are −17 and −27 kcal/mol, respectively, reflecting correctly the larger number of hydrogen bonds.

The snapshot in Figure 2 shows two water molecules forming obvious hydrogen bonds to imidazole, indicated by dashed lines. The water to N1–H bond has O···H = 1.90 Å, O···H–N1 = 153°, and an ON1C2N3 torsion angle of −169°. The bond to N3 has N3···H = 2.02 Å, N3···H-O = 156°, and ON3C2N1 = 106°. These values are consistent with the optimized geometric

(43) Hager, J.; Wallace, S. C. *J. Phys. Chem.* **1984**, *88*, 5513.
(44) Tubergen, M. J.; Levy, D. H. *J. Phys. Chem.* **1991**, *95*, 2175.
(45) Chou, P. T.; Martinez, M. L.; Cooper, W. C.; McMorrow, D.; Collins, S. T.; Kasha, M. *J. Phys. Chem.* **1992**, *96*, 5203.
(46) Suzuki, S.; Green, P. G.; Bumgarner, R. E.; Dasgupta, S.; Goddard, W. A., III; Blake, G. A. *Science* **1992**, *257*, 942.
(47) Novoa, J. J.; Tarron, B.; Whangbo, M. H.; Williams, J. M. *J. Chem. Phys.* **1991**, *95*, 5179.

parameters for the imidazole monohydrates (Table II). The Ow···H(N1) bond is shorter than the N3···Hw distance. The O···H···N angles are not very far from being linear. The Ow atom attached to H–N1 is almost in the plane of the ring. The OwN1C2N3 torsional angle indicates that the water oxygen hydrogen bound to the N3 site can be largely out of the plane of the ring. (See the discussion about the geometry of the Im-(3)W dimer using OPLS interaction potential.)

Characteristic points of the radial distribution functions (Table VIII) and the average geometric parameters (Table IX) can be well explained by considering the OPLS optimized dimers in Table II. All R_{max} values (R_{max} is the atom–atom separation where the radial distribution function has its first maximum) and average distances are larger by some hundredth of an angstrom than the optimal OPLS values in the dimer. This is due to the thermal motion at 298 K. Because of the steeper increase around its minimum of the intermolecular potential function toward smaller rather than larger molecular separations, the average distances of the atoms in hydrogen bonds are expected to be larger than their optimized value at 0 K. In fact, the absolute lengths of hydrogen bonds increased while the relative distances found in the dimers were maintained in solution. The (N1)H···Ow and the in-plane N1···Ow distances for imidazole are shorter by 0.1–0.2 Å than the N3···Hw and N3···Ow distances, respectively. The average N···H···Ow bond angles are more declined from linearity in the solution, reflecting configurations both with linear and bent hydrogen bonds. The average values are 172° and 171° for the N1···H···Ow and N3···H···Ow angles, while the optimal OPLS values are 178° and 177°, respectively (Table II). The average OwN3C2N1 torsion angle of 142° is very close to the optimal one of 141°. The value of 106° in Figure 2, however, suggests that, to obtain an average value above, the torsion angle must be close to 180° in some cases. Thus, owing to the insensitivity of the OPLS potential to this torsion, the water structure is poorly localized in the N3 region. In fact, the snapshot averaging shows that even the mostly populated oxygen and hydrogen positions comprise only the 31% and 20% of the total sample, respectively. Statistical analysis also shows poorly localized (population of the location sites are about 26%) water molecules with N1···Ow distances of about 3.5 Å. These water molecules are considered as hydrating in the π-region.

The characteristic points of the N1···Ow and H1···Ow radial distribution functions for pyrrole (Figure 4) and imidazole (Figure 5) are similar; thus the snapshot in Figure 2 may be considered as relevant also for the solution structure of pyrrole in the N1–H region. Water molecules in the π-region are at a distance of 3–4 Å from N1, a result coinciding with that obtained for the π-hydrated pyrrole in the gas phase.

The radial distribution functions in Figure 4 show a maximum for the N1···O separation at about 2.85 Å and for H1···Ow at 1.85 Å for pyrrole (Table VIII). (The radial distribution functions were monitored at a step size of 0.05 Å.) The difference is close to 0.95 Å, the O–H bond length in water. Similar difference was found for the R_{start} values, the smallest value where the $g(R)$ distribution function has a value of at least 0.01. Both differences can be met with nearly linear hydrogen bonds. The single snapshot (Figure 2) suggests hydration shell geometry close to that determined from the radial distribution functions. Averaging geometric data in 4000 snapshots for imidazole (Table IX) also predicts a nearly linear hydrogen bond to H–N1 with Ow in the molecular plane and with a H···Ow distance of 1.81 Å.

The peaks are higher and narrower for imidazole (Figure 5) than for pyrrole both in the N1···Ow and H1···Ow radial distribution functions. This suggests more localized water in the N1–H region with imidazole solute even though the coordination number, 1, is the same for both solutes considering the whole hydration shell (Table VIII). This is in line with the more negative binding energy for Im(1)W than for PyWσ. The value of 0.8 for the number of hydrogen bonds to pyrrole means that not all water molecules in the first hydration shell are hydrogen bonded to the solute; rather only about 80% are. Values for the number of hydrogen bonds smaller by some tenths of units than the coordination number have been found for several solutes in aqueous solution.[19,48] Considering that the solute–solvent interactions with energy more negative than –3.5 kcal/mol contain contributions from waters also in the π-region, the fraction of the configurations when the water molecules are in-plane hydrogen bonding to the N1–H bond is presumably less than 80%. This is in line with our statistical result for the imidazole that only 64% of snapshots showed water bound to the N1–H bond of the solute.

The number of the hydrogen bonds for imidazole is 1.8. Assuming that there are 0.64 (64%) in-plane bonds to N1-H, there remain about 1.2 bonds to other sites, namely, to N3 and to the π-region. This is reasonably less than the N3/Hw and N3/Ow coordination numbers, both of which are 1.4. The differences of the corresponding R_{start} and R_{max} values in the N3···Hw and N3···Ow radial distribution functions are about 0.95–1.00 Å, almost the O–H bond length in water. These values suggest linear hydrogen bonding also to the N3 site in accord with the OPLS predicted N3···H–O angle for Im(3)W (see Table II).

Analysis of the solution structure around the polar sites of the protonated imidazole solute is much simpler than that for the neutral molecules. The snapshot in Figure 7 indicates two water molecules as acceptors in hydrogen bonds to N1–H and N3–H. The H···Ow bond lengths are 1.63 Å and 1.85 Å, close to the MP2 and OPLS optimized distances for ImH^+W in the gas phase. The Ow···H–N angles are 161° and 147°, showing usually and somewhat more bent hydrogen bonds. There are several water molecules above and below the ring oriented with the O facing the ionic solute. N···O distances for these waters are 3–4 Å.

The energy pair distribution function (Figure 3) has a single maximum in the range of –17 to –9 kcal/mol. The most negative interaction energy coincides with the OPLS optimized energy of –16.7 kcal/mol in the ImH^+W monohydrate. Integration up to –9 kcal/mol reveals two hydrogen bonds. These are considered as N–H···Ow bonds as are shown in the snapshot. The solute–solvent interaction energy is –119 kcal/mol, larger by an order of magnitude than that for the neutral species. If the Born correction is used[49] to account for the interaction with the solvent beyond the cutoff radius of 9.75 Å, the E_{SX} value is –135 kcal/mol.

N···Ow and H···Ow radial distribution functions (Figure 4) have maxima at 2.70 Å and 1.75 Å, respectively, at somewhat smaller distances than the neutral molecules do. This indicates stronger interaction of the solvent with the ionic solute. The peaks are considerably higher and narrower, showing more strictly localized waters around the imidazolium ion. There is a large second peak in the N···Ow curve at about 4.8 Å, considered the contribution from water molecules hydrating the other N–H area. Similar effects were found with another bifunctional molecule, 1,2-ethanediol.[19]

The OPLS potential function predicts nearly linear hydrogen bond for ImH^+W in the gas phase. The sum of the R_{max} value for H···Ow and the N–H distance of 1.018 Å for imidazolium cation (Table I) is 2.768 Å, much larger than the R_{max} value 2.70 Å for N···O. This inequality predicts, on average, a more bent hydrogen bond structure in solution than in the monohydrate. Remarkable deviation from linear hydrogen bonding obtained in simulations for aqueous solution is quite general, as was reviewed recently.[48]

Information about the solution structure in the nonpolar regions can be obtained by analyzing the C2···Ow and C4···Ow radial distribution functions (Figure 6 and Table VIII). R_{start} values are uniformly about 2.9 Å. The R_{max} for the C2···Ow curve is at 3.75 Å for imidazole. A higher and narrower first peak at 3.6

(48) Nagy, P. I. *Acta Chim. Hung.* **1992**, *129*, 429.
(49) Jorgensen, W. L.; Blake, J. F.; Buckner, J. K. *Chem. Phys.* **1989**, *129*, 193.

Å for the imidazolium cation indicates a more structured solvation shell around the C2 atom of the pronated ring. Because the C2 atom is between two polar atoms in the ring, water molecules in the first hydration shells of the polar sites contribute to the first peaks of the C2···Ow curves. This is more evident when comparing with the remarkably shorter and broadened first peaks in the C4···Ow radial distribution functions. The reason for the change in the shape of the peaks is that the C4 atom has only one polar ring nitrogen neighbor. The C4···Ow first peak for imidazole is the shortest and flattest of the curves in Figure 6. Since C4 is neighboring the N3 atom of the ring, the least ordered solvent structure around the imidazole C4 is indirect evidence of the reduced ability of the N3 site to locate water molecules strongly. Coordination numbers are also in line with the above interpretation. The C2/Ow values are 10 both for the neutral and ionic solutes. The C4/Ow value of 9 is only slightly decreased for the imidazolium solute, reflecting the strong localizing ability of even a single NH group. The C4/Ow is more reduced for imidazole according to a less ordered structure around N3.

An interesting feature of the C4···Ow radial distribution functions are the well-defined second maxima at 4.8-5.0 Å. They are similar to each other and are definitely sharper than the first C4···Ow peak for imidazole. These second peaks are explained as reflecting the ordered structure around the N1 atom of the rings. The C4···N1 distance is nearly the same in both rings; thus the similar location for the second peaks is reasonable.

The first peak of the C2···Ow radial distribution function for pyrrole (not indicated) is located at the same value, $R = 3.75$ Å, as that for imidazole. The R_{max} is larger by about 0.1 Å than the comparable peak sites for simple aliphatic systems with polar groups.[16,19,48] Owing to the lack of a second polar neighbor to C2 in pyrrole, the peak is considerably broader than in the case of imidazole. The curve reaches a minimum only at 5.00 Å. Accordingly, the C2/Ow coordination number is increased to 14. Difference in the C2···Ow and C4···Ow R_{max} values emphasizes the contribution from water molecules solvating the polar site. The C4 (or C3) atom in pyrrole is the only carbon atom β to a polar group in the systems investigated here. R_{max} of the C4···Ow curve is shifted toward larger values, reflecting the reduced contribution from water molecules close and strongly bound to the polar site. There is a second, sharp peak in the pyrrole C4···Ow curve at about 5.0 Å, leading to the same interpretation as above for the structured solvation shell around the polar site. This second peak close to 5 Å, common to all three solutes here, results in R_{min} values for the C4···Ow curves smaller than for the C2···Ow radial distribution functions.

Conclusions

Ab initio calculations were carried out in the gas phase for water, pyrrole, imidazole, and protonated imidazole monomers and different monohydrates formed of them. Total geometry optimization at MP2/6-31G* level has given geometries for the ring systems in good agreement with experimental geometries. Normal frequencies calculated at HF/6-31G* and MP2/6-31G* levels are systematically overestimated. By calculating the free energies of the monomers at 298 K and 1 atm, the gas-phase protonation energy of imidazole was estimated. Using MP2/6-311++G** single point calculations, the protonation energy was obtained with a difference of 2.3 kcal/mol referred to the experimental value. Calculations of the free energies of the water···ring system complexes allowed us to estimate the relative populations of the monohydrates with different geometries. Hydration of pyrrole in the plane is preferred by 1.8 kcal/mol over the out-of-plane hydrated form. The in-plane hydration of the imidazole ring is favored by 1.7 kcal/mol at the N1 site as compared to the N3 site. The protonated imidazole forms a stable in-plane hydrate with an N–H···Ow hydrogen bond.

Gas-phase monohydrates optimized at the HF level have hydrogen bond distances longer by about 0.1 Å than the MP2 values. Using the OPLS interaction potential the bond distances were shorter than the MP2 values by 0.02–0.17 Å. While the hydrogen bond angles from all three methods are close, the OPLS interaction potential allows strongly out-of-plane hydration at the N3 site of imidazole, in contrast to the ab initio results. Relative dimerization energies with the OPLS potential are close to the BSSE corrected MP2/6-31G* values. The only remarkable exception is the hydration of the neutral imidazole at the N3 site. In general, the OPLS potential which was developed to give good calculated thermodynamic measurables predicts reasonable hydrogen bond structure and relative hydration energies for pyrrole, imidazole, and protonated imidazole. The OPLS generated geometric parameters and relative energies of monohydrates are closer to the ab initio MP2/6-31G* than HF/6-31G* values.

Geometric structure parameters in the first hydration shells of the polar sites are consistent with those obtained for monohydrates optimized using OPLS interaction potential function. The thermal motion considered in the solution simulation results in average hydrogen bond distances longer by some hundreths of an Å than the corresponding gas-phase values. The N···H···O angles are about 170° on average, allowing both linear and bent hydrogen bonds.

The pyrrole molecule forms a strong hydrogen bond of N-H···Ow type in the molecular plane. The neutral imidazole forms approximately two hydrogen bonds; one hydrogen bond is formed to the N1 site with N1–H···Ow in the ring plane. Other water molecules which hydrate the N3 site and are located in the π-region form weaker bonds to the solute. The nonpolar parts of the rings are hydrated by several molecules with the largest probability at distances of 3.7–3.9 Å from the ring carbon atoms. The protonated imidazole forms two strong in-plane hydrogen bonds of N-H···Ow type in aqueous solution. According to a snapshot there are several water molecules in the π-region facing with oxygen to the ring. The solution is more structured in the C–C region with charged than with neutral solute.

The statistical perturbation method used in Monte Carlo simulations predicted relative solvation energy values. The free energy of solvation for imidazole relative to pyrrole is –4.1 kcal/mol. The relative solution enthalpy and entropy are –10 to –12 kcal/mol and –6 to –8 kcal/mol, respectively.

Acknowledgment. The authors are thankful to Dr. W. L. Jorgensen for providing the BOSS 3.1 program and to Dr. W. J. Dunn III for providing the statistical analysis program. We thank Cambridge Neuroscience for financial support. D.A.S. acknowledges Molecular Simulation, Inc., for a grant of software including the AVS Chemistry Viewer and the Ohio Supercomputer Center for a grant.

Note Added in Proof. A very recent paper of Sadlej et al.[50] and a former one by Fan et al.[51] discuss the vibrational spectra of imidazole based on ab initio calculations using the 4-21G basis set. Both papers find discrepancies in the theoretical assignations of the vibrations as compared to the experimental frequencies and assignations. These theoretical results indicate a need to consider the experimental values (a selection is given in Table III) with caution.

(50) Sadlej, J.; Jaworski, A.; Miaskiewicz, K. *J. Mol. Struct.* **1992**, *274*, 247.

(51) Fan, K.; Xie, Y.; Boggs, J. E. *J. Mol. Struct. (THEOCHEM)* **1986**, *136*, 339.